

# Biocidal Properties of a Glycosylated Surface: Sophorolipids on Au(111)

Claire Valotteau,<sup>†,‡</sup> Christophe Calers,<sup>‡</sup> Sandra Casale,<sup>‡</sup> Jan Berton,<sup>§</sup> Christian V. Stevens,<sup>§</sup> Florence Babonneau,<sup>†</sup> Claire-Marie Pradier,<sup>‡</sup> Vincent Humblot,<sup>\*,‡</sup> and Niki Baccile<sup>\*,†</sup>

<sup>†</sup>Sorbonne Universités, UPMC Univ Paris 06, CNRS, Collège de France, Laboratoire de Chimie de la Matière Condensée de Paris, UMR 7574, 11 Place Marcelin Berthelot, 75005 Paris, France

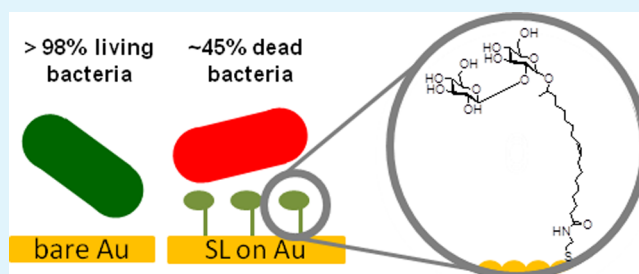
<sup>‡</sup>Sorbonne Universités, UPMC Univ Paris 06, CNRS, Laboratoire de Réactivité de Surface, UMR 7197, 4 Place Jussieu, 75005 Paris, France

<sup>§</sup>SynBioC Research Group, Department of Sustainable Organic Chemistry and Technology, Faculty of Bioscience Engineering, Ghent University, Coupure Links 653, B-9000 Gent, Belgium

## S Supporting Information

**ABSTRACT:** Classical antibacterial surfaces usually involve antiadhesive and/or biocidal strategies. Glycosylated surfaces are usually used to prevent biofilm formation via antiadhesive mechanisms. We report here the first example of a glycosylated surface with biocidal properties created by the covalent grafting of sophorolipids (a sophorose unit linked by a glycosidic bond to an oleic acid) through a self-assembled monolayer (SAM) of short aminothiols on gold (111) surfaces. The biocidal effect of such surfaces on Gram+ bacteria was assessed by a wide combination of techniques including microscopy observations, fluorescent staining, and bacterial growth tests. About 50% of the bacteria are killed via alteration of the cell envelope. In addition, the roles of the sophorose unit and aliphatic chain configuration are highlighted by the lack of activity of substrates modified, respectively, with sophorose-free oleic acid and sophorolipid-derivative having a saturated aliphatic chain. This system demonstrates thus the direct implication of a carbohydrate in the destabilization and disruption of the bacterial cell envelope.

**KEYWORDS:** *sophorolipid, glycolipid, surface functionalization, self-assembled monolayer, antibacterial coating, killing-by-contact, biocidal mechanism*



## INTRODUCTION

Biological contamination of surfaces is a major concern in the medical and pharmaceutical industries,<sup>1</sup> food-processing installations, water pipes, naval ships, as well as in monuments and cultural heritage materials. Bacteria, fungi, or algae are inclined to adhere and grow onto solid surfaces, leading to the formation of biofilms<sup>2</sup> that may lead to undesired phenomena like loss of adhesion properties, degradation, or infection. Surface contamination has an important socio-economical impact. For instance, nosocomial infections in the U.S.A. were estimated to 1.7 million in 2002 and leading to slightly less than 100 000 death cases.<sup>3</sup> Moreover, bacteria in biofilms are generally more resistant,<sup>4</sup> thus making the antibiotics ineffective in the long run. To prevent these problems, a large amount of research is carried out to develop preventive antimicrobial coatings on surfaces, including either antiadhesive or biocidal strategies. In the latter, one mainly finds either a killing-by-contact<sup>5</sup> or a killing-by-release<sup>6</sup> approach, where the active compound can be antibiotics,<sup>7</sup> quaternary ammonium derivatives,<sup>5</sup> nanoparticles,<sup>8</sup> etc., either blended into or deposited onto a substrate<sup>9</sup> or chemically grafted onto surfaces.

Nevertheless, the ecotoxicity of most of these compounds, the increasing resistance of microorganisms, or the complexity of the grafting strategy restrict their practical use at large scales. Bioderived compounds, e.g., enzymes, molecules able to interfere with quorum-sensing phenomena, or antimicrobial peptides, appear as appealing alternatives for their broad range of action, their efficiency at very low concentration, and the absence of bacterial resistance. However, their high cost of synthesis and purification, pH sensitivity, susceptibility to proteolysis, as well as potential local toxicity and allergy after repeated applications may restrict their use.<sup>10</sup>

In this context, carbohydrates, one of the most common compounds in living systems, are of increased interest for a large number of medical and pharmacological-related applications, like vaccines and anticancer drugs,<sup>11</sup> fabrication of glycoarrays for antibody recognition and cell adhesion,<sup>12</sup> antibiofilm and antimicrobial formulations,<sup>13</sup> just to cite some. Even if

Received: June 10, 2015

Accepted: July 28, 2015

Published: August 6, 2015

carbohydrates alone are a source of nutrition to microorganisms rather than biocidal compounds, some reports relate the antimicrobial effects of sugar-containing molecules, such as bacterial exopolysaccharides, extracted from *Escherichia coli*,<sup>14</sup> and few glycoconjugates, carbohydrates covalently linked to an organic moiety (from simple alkyl chain to more complex structures), of both synthetic and natural origins. For instance, amphotericin B, a complex glycolipid extracted from *Streptomyces nodosus*, is used to treat fungal infections<sup>15</sup> and other compounds display interesting antimicrobial properties.<sup>13</sup> Until now, only two forms of antimicrobial actions of carbohydrate derivatives have been described: (1) a biocidal action via cellular lysis promoted by glycolipids in solution,<sup>13</sup> (2) an antiadhesive effect, commonly observed for polysaccharides and glycolipids either immobilized on a substrate (glycoarray) or free in solution.<sup>13,16–20</sup> Even though the mechanisms of action are still largely debated, the biocidal action is likely due to the amphiphilic nature of the glycolipids, which penetrate into the plasma membrane, causing lysis and possible leakage of cytoplasm material.<sup>21–23</sup> Since neither pure carbohydrates, nor most common lipids, like fatty acids,<sup>24</sup> have specific biocidal properties, one generally refers to as a “surfactant effect”, where the role in the membrane lysis cannot be attributed to a specific part of the molecule but rather to its physicochemical properties in solution.<sup>25,26</sup> In terms of the antiadhesive effect, this is believed to depend on competing protein–sugar interactions between the pathogen and the substrate, where proteins refer to carbohydrate-binding proteins like lectins and adhesins present in the cell envelope. Playing with the nature of a carbohydrate coating (type, mobility, number of sugars), one can either increase or reduce the affinity of cells for a surface, thus promoting, or discouraging, cell adhesion phenomena.<sup>16–18</sup>

In the context of carbohydrate-driven antimicrobial activity, we show here the first example of a glycosylated surface with biocidal properties. To do so, we use sophorolipids (SL), a family of bolaform glycolipids characterized by a sophorose unit (glucose  $\beta(1-2)$ ), linked through a glycosidic bond to oleic acid (Figure 1) and having a COOH group free of access for chemical grafting at the opposite side of the carbohydrate. Sophorolipids are characterized by a low toxicity, high biodegradability and an environmental compatibility and possess both antifungal and/or antimicrobial properties in solution.<sup>13,27,28</sup> They are produced in large amounts by the yeast *Starmerella bombicola*,<sup>29</sup> they are already commercialized

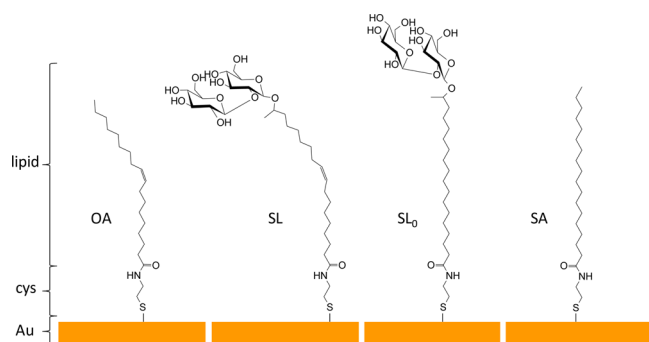


**Figure 1.** Functionalization of gold surfaces with oleic acid (OA), acidic monounsaturated sophorolipid (SL), acidic fully saturated sophorolipid ( $SL_0$ ), and stearic acid (SA). Cysteamine (cys) constitutes the primer for all compounds.

worldwide (e.g., Soliance, Ecover, IntoBio, Saraya),<sup>30</sup> and probably the most interesting feature, they are ready as-such, needing no specific chemical synthesis nor complex protection/deprotection modification. They constitute an ideal platform for large-scale antimicrobial surface applications, if compared to competitors like antimicrobial peptides or customized glycoconjugates. In addition, our approach demonstrates the direct involvement in the cell envelope-destabilization/disruption of a carbohydrate, the role of which is largely debated in the biocidal properties of glycolipids in solution<sup>31</sup> but also in the more general context of carbohydrate/lipidic membrane interactions.<sup>32</sup>

The open acidic form of sophorolipids (SL) will be grafted on model flat gold (111) surfaces using short thiolamines as primers (cysteamine, cys). The modified gold surfaces are characterized step by step by polarization-modulation reflection absorption infrared spectroscopy (PM-RAIRS) and X-ray photoelectron spectroscopy (XPS). Antimicrobial activity is tested against *Listeria ivanovii*, a Gram positive bacterium, surrounded by a thick peptidoglycan layer without an outer membrane, since sophorolipids appear more effective in solution against bacteria exhibiting such a cell envelope. Antimicrobial properties are qualitatively and quantitatively evaluated through a combination of atomic force microscopy (AFM) and scanning electron microscopy with a field emission gun (SEM-FEG), fluorescent staining, and bacterial growth tests and compared to blank samples constituted by the gold surface alone and the cysteamine-modified gold surface. In order to elucidate the role of the sophorose group in the biocidal action, we develop and graft on control gold surfaces three SL-related molecules, either bearing the same sugar but a different chain or playing with the chain without sugar (Figure 1): (1) oleic acid (OA), which mimics only the aliphatic chain of sophorolipids, (2) a sophorolipid-derivative having a fully saturated aliphatic chain ( $SL_0$ ), important to observe the possible role of the molecular conformation at the gold surface due to the presence of a C=C double bond, and (3) stearic acid (SA), which mimics the aliphatic chain of the fully saturated sophorolipid-derivative.

## MATERIALS AND METHODS

Cysteamine (cys), *N*-hydroxysuccinimide (NHS), 1-(3-(dimethylamino)propyl)-*N*-ethylcarbodiimide hydrochloride (EDC), oleic acid (OA), stearic acid (SA), formaldehyde, dimethyl sulfoxide, and sodium chloride (NaCl) were obtained from Sigma-Aldrich (Saint Quentin Fallavier, France). Sophorolipids (SL) were derived from a commercial acidic and lactone mixture of sophorolipids purchased from Soliance (France) (Sopholiance S; batch number, 11103A; dry content,  $60 \pm 6\%$ ). To obtain a high purity ( $>92$  mol %, by <sup>1</sup>H NMR) form of the nonacetylated acidic sophorolipids only, we employed a classical hydrolysis route using 5 M NaOH followed by acidification by HCl and pentanol extraction (please refer to ref 33 for more details) of the sophorolipid only. The fully saturated sophorolipid compound ( $SL_0$ ) was derived from the previous one using a Pd-catalyzed hydrogenation reaction described in ref 34. All solvents were reagent-grade and were used without any further purification. Water was purified with a Milli-Q system (Millipore, resistivity  $>18$  M $\Omega$  cm<sup>-1</sup>) from EMD Millipore Corp. (Billerica, MA). Glass substrates, coated successively with a 50 Å thick layer of chromium and a 200 nm thick layer of gold, were purchased from Arrandee (Werther, Germany).

**Surface Preparation.** The substrates have been prepared using a standard protocol.<sup>35</sup> Prior to use, the gold-coated substrates were annealed in a butane flame to ensure a good crystallinity of the top layer, after what they were exposed to UV-ozone during 15 min and

rinsed successively in a bath of ultrapure water and in a bath of absolute ethanol during 10 min. First, the substrates were immersed in an ethanolic solution of cys at 10 mM. After 3 h, the substrates were sonicated in ultrapure ethanol to desorb the nongrafted molecules and thoroughly rinsed in ethanol and then in ultrapure water before being dried under a flow of dried air. Next, to promote the grafting of the SL on the thiol-amine, the carboxylic acid termination of SL (50 mg L<sup>-1</sup>) was activated by succinimide ester using a mixture of EDC (77 mg L<sup>-1</sup>) and NHS (23 mg L<sup>-1</sup>) in water. After 1 h under stirring, the cys-modified gold substrates were immersed for 3 h in this solution. Successive rinsing in ultrapure water and ethanol were performed to remove noncovalently grafted reactants before drying under a flow of dried air. A quartz crystal microbalance was used to verify that the rinsing procedure efficiently eliminated the excess of unreacted SL. OA, SA, and SL<sub>0</sub> were grafted onto gold following a similar protocol, using ethanol as solvent. The as-obtained surfaces are depicted in Figure 1. All samples were characterized by PM-RAIRS and XPS after each step of functionalization.

**Characterization Techniques. Polarized Modulated Reflection Absorption Infrared Spectroscopy (PM-RAIRS).** PM-RAIRS measurements were performed using a Nicolet Nexus 5700 FT-IR spectrometer equipped with a nitrogen-cooled HgCdTe wide band detector. Infrared spectra were recorded at 8 cm<sup>-1</sup> resolution, by coaddition of 128 scans. A ZnSe grid polarizer and a ZnSe photoelastic modulator were placed prior to the sample in order to modulate the incident beam between p and s polarizations (HINDS Instruments, PM90, modulation frequency = 36 kHz). The sum and difference interferograms were processed and underwent Fourier-transformation to yield the PM-RAIRS signal which is the differential reflectivity ( $\Delta R/R^{\circ}$ ) = (Rp - Rs)/(Rp + Rs), where Rp is the signal parallel to the incident plane while Rs is the perpendicular contribution. The measurements were done at two different voltages applied to the modulator ZnSe crystal to optimize the sensitivity.

**Infrared-Attenuated Total Reflection (IR-ATR).** IR-ATR measurements were recorded using a Nicolet 5700 FT-IR spectrometer equipped with a nitrogen-cooled MCT detector. Infrared spectra were obtained by coadding 256 scans at 8 cm<sup>-1</sup> resolution and referencing against the background of air.

**Atomic Force Microscopy Imaging (AFM).** AFM images of dried surfaces were recorded using a Caliber AFM microscope from Bruker Instruments Inc. Topographic images were taken in the tapping mode. Silicon nitride tips (resonance frequency 280–400 Hz, force constant 40–80 N/m) have been used. Images were obtained with a constant speed of 1 Hz with a resolution of 512 lines and 512 pixels each. The raw data were processed using the imaging processing software Nanoscope Analysis v.1.30 from Bruker (Nano Surfaces Corp. Santa Barbara, CA) and used mainly for slope corrections.

**Scanning Electron Microscopy with Field Emission Gun (SEM-FEG).** SEM images were recorded with a Hitachi SU-70 field emission gun scanning electron microscope. The samples were fixed on an alumina SEM support with a carbon adhesive tape and were observed without metallization. An in-lens secondary electron detector (SE-Upper) was used to characterize our samples. The accelerating voltage was 1 kV, and the working distance was around 5 mm. At least five different locations were analyzed on each surface, arising to the observation of a minimum of 100 single bacteria observed.

**Water Contact Angle Measurements.** Static water contact angles were measured under ambient conditions (at 20 °C and 40% relative humidity) analyzing the drop profile of sessile drops. A 10 μL droplet of milliQ water was deposited on the sample surface using a Krüss DSA100 apparatus (Germany) equipped with a CCD camera and an image analysis processor. Four droplets were analyzed on different locations on each sample, and the test was performed in triplicate on three different samples. The reported values are the averages of these 12 measurements for each kind of surface.

**Molecular Drawing of SL and SL<sub>0</sub> on a Flat Surface.** Sophorolipid SL and SL<sub>0</sub> molecules covalently bonded on cysteamine via an amide bond had been drawn respecting bond lengths, dihedral angles, and sense of chirality for each atom. We referred to the IUPAC name for sophorolipids: 17-L-[(2-O-β-D-glucopyranosyl-β-D-glucopyranosyl)-

oxy)-octadecenoic acid. Drawing and structure relaxation was done with the Gaussview software, version 2.1 while the images have been done using the PyMOL molecular graphic system, version 1.3.

**Antimicrobial Activity. Strains and Culture Conditions.** Non-human pathogenic bacteria *Listeria ivanovii* Li 4pVS2 were used to investigate the modified surfaces. Unless otherwise indicated, bacterial suspensions were always prepared from stationary phase cultures incubated overnight in brain heart infusion (BHI) broth (BD Difco, France) at 37 °C under agitation (250 rpm). The broth was then centrifuged at 10 000g for 5 min, the supernatant was eliminated, and the bacteria were redispersed in an isotonic sterile solution (NaCl 0.9%). The optical density of the broth was controlled at 620 nm and adjusted at 0.05, which corresponds to 5 × 10<sup>6</sup> colony forming unity (CFU) per mL.

**Deposition of Bacteria on Samples.** A 100 μL drop of bacteria solution freshly prepared was deposited on each surface sample, which were previously washed in a 70% ethanol aqueous solution and dried in sterile environment. In all experiments, unless otherwise mentioned, the inoculated surfaces were incubated for 3 h at room temperature under a wet atmosphere.

**Evaluation of Bacteria Adhesion by Infrared Spectroscopy.** After bacterial deposition and incubation during 3 h, surfaces were washed five times with 100 μL drops of isotonic sterile solution (NaCl 0.9%) and dried under a laminar air flow. A total of 10 infrared spectra were acquired by PM-RAIRS on each sample in order to scan their entire surface and collect the signal from all the adhered bacteria. All measurements (on bare gold and modified surfaces) had been done during the same experimental session, thus reducing at minimum intensity variations of the background, beam intensity and alignment. The relative amounts of bacteria adsorbed were evaluated by considering the amide bands area, the bacteria IR fingerprints. The areas were integrated from 1700 to 1500 cm<sup>-1</sup> to include the whole signal due to amides I and II contributions, respectively, at 1660 and 1550 cm<sup>-1</sup>. The attachment of bacteria onto the different surfaces is expressed as a percentage compared to gold substrates: Ad(%) = 100 × (area of amide bands on sample)/(area of amide bands on gold). The uncertainty attached to this percentage comes from the propagation of the uncertainties attached to the measurement of amide bands area on both the considered surface and the gold substrate. These results were confirmed by repeating the same procedure above on three different set of samples.

**Observation of Bacterial Morphology by Microscopy.** Qualitative analysis of the bacterial morphology was done by mean of AFM and SEM-FEG microscopies, which enables one to visualize the effect of antimicrobial products on bacteria and could help to identify general target sites.<sup>25</sup> Since SEM-FEG observations are done under vacuum, samples were previously treated as follows: after the incubation period, 12 μL of formaldehyde at 37% were added in order to fix the bacteria and avoid collapsing of bacteria upon drying. After 15 min, samples were washed six times with 100 μL drops of filtered ultrapure water to remove nonadhered bacteria and dried under a laminar air flow.

**Evaluation of Bacteria Viability by Fluorescent Staining.** Damaged bacteria on the surface were counted using the Live/Dead Bacterial Viability Kit (BacLight). In total, 1.5 μL of each fluorescent stain, Syto9 and propidium iodide (PI), were added to 1 mL of ultrapure water. After incubation, surfaces were rinsed five times using 100 μL drops of an isotonic sterile solution and 10 μL of the fluorochrome solution were deposited on the surfaces. Samples were then left during 10 min in dark and at room temperature prior to microscopy analysis. Surfaces were always kept under a humid environment during the whole time of the experiments to avoid water evaporation. Samples were then examined with an epifluorescence microscope (AXIO 100 Zeiss). Images were acquired with a 10× or 40× objective lens and recorded with a CCD camera (AxioCam MRm Zeiss). Fluorochromes were, respectively, excited and detected at 455–495 nm and 505–555 nm (for Syto9) and at 533–558 nm and 570–640 nm (for PI). About 10 different locations of each surface were analyzed in order to have statistically relevant data; this experiment was conducted on three sets of samples and at least a thousand of bacteria were then enumerated. Bacterial counting (red,

damaged membrane; green, intact membrane) was done using the software ImageJ and the viability is calculated as follows:  $\text{Viability}(\%) = 100 \times (\text{number of green bacteria}) / (\text{number of green bacteria} + \text{number of red bacteria})$ .

**Bacteria Growth Capacity.** The evaluation of bacterial growth capacity after being in contact with the samples completes the characterization data set and was done as follows: after bacterial deposition and incubation during 3 h, the surfaces were washed five times with 100  $\mu\text{L}$  drops of isotonic sterile solution. Samples were then transferred into a sterile tube containing 2 mL of isotonic sterile solution (NaCl at 0.9%) and sonicated 5 min. The gold sample was removed and bacteria suspensions were diluted 100 and 1000 times. A volume of 50  $\mu\text{L}$  of each dilution was deposited in duplicate on Petri dishes filled with BHI agar (15 g/L). The plates were incubated at 37  $^{\circ}\text{C}$  overnight before enumeration. Results are expressed in percentages of the number of attached and cultivable bacterial cells onto the different surfaces as compared to gold substrates:  $\text{Growth}(\%) = 100 \times (\text{number of colonies forming unity on sample}) / (\text{number of colonies forming unity on bare gold substrate})$ . These tests were done in triplicate on each type of samples and the percentage of growth was averaged over the three samples. The uncertainty attached to these results follows from the statistical analysis of these repeated experiments.

**Minimum Inhibitory Concentration (MIC) and Minimum Bactericidal Concentration (MBC) Determination.** The MIC values of sophorolipids and derivatives used for surface grafting were determined using a liquid growth inhibition assay. An exponential-phase bacterial culture of *Listeria ivanovii* was diluted in broth to an optical density of 0.01 ( $10^6$  CFU/mL). A volume of 50  $\mu\text{L}$  of this bacterial suspension were mixed with 50  $\mu\text{L}$  of 2-fold serial aqueous dilutions of each product (final concentrations of sophorolipids and derivatives from 2 to 32 mg/mL). As OA, SA, and SL<sub>0</sub> are not soluble in water, these products were first solubilized into 10% of DMSO. The bacterial growth was monitored by measuring the change in optical density. This test was performed in triplicate with positive (0.7% formaldehyde) and negative (isotonic solution) inhibition controls. MIC is expressed as the lowest concentration that completely inhibits bacterial growth after overnight incubation.

The bacterial suspension with a concentration of sophorolipid superior or equal to the MIC are diluted and deposited on the agar plate in order to determine the minimum bactericidal concentration (MBC). The MBC is expressed as the lowest concentration for which no colony forming unit are observed on agar plates after overnight incubation.

## RESULTS

**SL Grafting on Au(111).** Figure 2 shows the PM-RAIRS spectra of gold surfaces after each functionalization step. After treatment in the cysteamine solution and rinsing, a typical IR spectrum of aminothiols is observed, with the expected absorption bands of NH and CH<sub>2</sub> groups as described in the literature.<sup>35</sup> The grafting of cysteamine is also confirmed by XPS analyses (bottom spectra in Figure S1 in the Supporting Information). Then, the PM-RAIRS spectrum of the SL-modified sample (Au-cys-SL) shown in Figure 2 exhibits the typical vibrations expected for SL, as shown by the comparison with the corresponding IR-ATR powder spectrum as well as the signature of the amide group at 1648  $\text{cm}^{-1}$  ( $\nu_{\text{C=O}}$ ) and 1538  $\text{cm}^{-1}$  ( $\nu_{\text{CN}}$  and  $\delta_{\text{NH}}$ ). These results confirm that the SL molecules are covalently grafted on the outer NH<sub>2</sub> group of cysteamine via an amidation reaction with the COOH moiety of SL. They are corroborated by XPS spectra recorded on the Au-cys-SL sample (top spectra in Figure S1 in the Supporting Information). The additional weak band at 1738  $\text{cm}^{-1}$  on the PM-RAIRS spectrum of Au-cys-SL, ascribed to a  $\nu_{\text{C=O}}$  vibration, may indicate the presence of spurious amounts of either NHS or NHS-activated sophorolipid despite rinsing. The

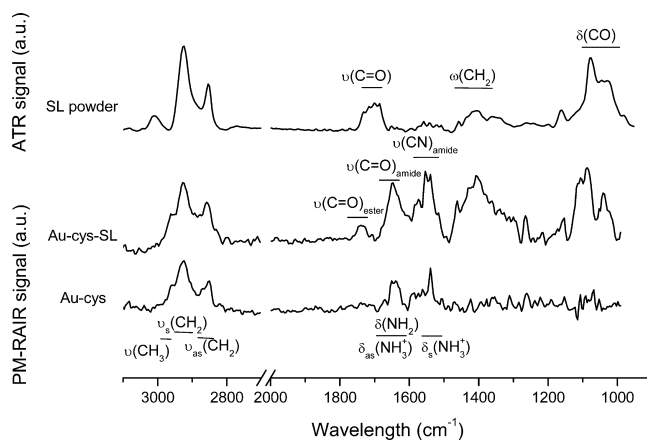


**Figure 2.** IR-ATR spectrum of the monounsaturated acidic sophorolipid powder (SL powder) and PM-RAIRS spectra of the cysteamine (Au-cys) and SL-grafted surfaces (Au-cys-SL) with identification of the main contributions.

rinsing step enables yet to eliminate at best the poorly attached molecules and to obtain a stable layer, as shown by quartz crystal microbalance experiments (cf. Figure S2 in the Supporting Information).

### Antimicrobial Activity. Surface Antimicrobial Properties.

In order to evaluate the antimicrobial activity of the SL-functionalized gold surfaces, we have combined AFM, SEM-FEG with epifluorescence microscopy, and microbial viability tests, on both SL-modified (Au-cys-SL) and SL-free gold surfaces (Au and Au-cys). SEM-FEG is a fast screening technique to evaluate eventual morphological changes of the microorganisms. To avoid possible artifacts due to vacuum conditions, bacteria have been fixed on the wet surfaces with formaldehyde, known to cross-link the membrane proteins in their current state. Moreover, we always deposit bacteria on bare gold substrate as a control sample. On the contrary, imaging by AFM, a noninvasive microscopy technique commonly used to explore mechanical stress on biointerfaces, was performed on as deposited, non-cross-linked, bacteria under ambient temperature and pressure conditions.

AFM and SEM-FEG images in Figure 3 show *L. ivanovii* deposited on SL-free samples (Au and Au-cys). Bacteria are of about 1  $\mu\text{m}$  in length and exhibit the expected elongated rod shape.<sup>36</sup> On the SEM-FEG image, the plasma membrane of the Gram+ bacteria appears as a white line surrounding the ovoidal shape of the microorganism indicating that contact with these surfaces does not alter the cell envelope. On the contrary, on the SL-modified surfaces (Au-cys-SL), bacteria do not have their native oval shape and the cell envelopes are damaged and appear pierced, causing the leakage of the cytoplasmic content and the collapse of the bacteria, as indicated by the arrows in Figure 3 (Au-cys-SL). These observations show direct evidence that the gold surface, grafted with SL, damages the plasma membrane of *L. ivanovii* in agreement with the antibacterial effect reported for sophorolipids in solution.<sup>23,28,37</sup>

To confirm these findings and quantify the number of damaged bacteria, bacterial staining with fluorescent markers, Syto9 and PI, was conducted in such way that green-stained bacteria indicate an intact plasma membrane, while red-stained bacteria show a damaged cell membrane. Our results show that less than 5% of bacteria are damaged on both Au and Au-cys surfaces while almost half of the bacteria population has a damaged membrane on the Au-cys-SL sample (Figure 3).

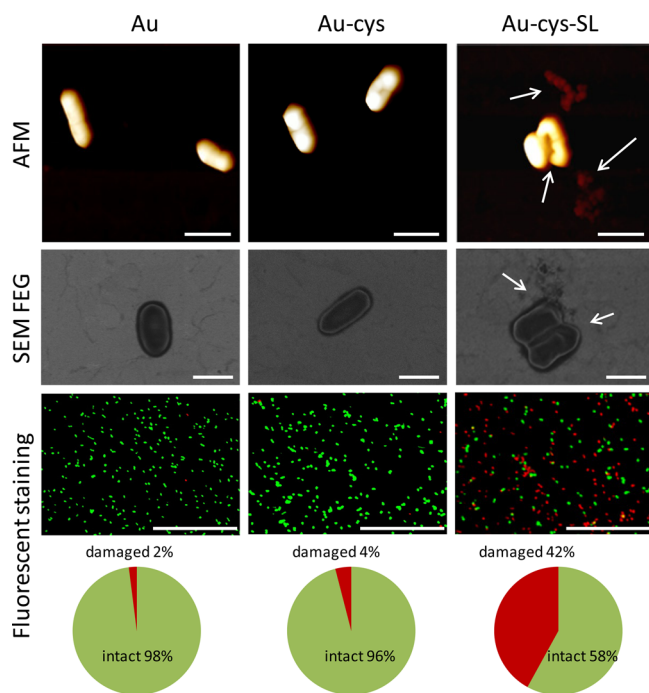


**Figure 3.** Bacteria (*L. ivanovii*) deposited on Au (left column), Au-cys (middle column), and Au-cys-SL (right column) surfaces observed by AFM (top range), SEM-FEG (middle range), and epifluorescence microscopy (bottom range). The charts below each image represent the percentage of adhering intact and damaged bacteria according to fluorescent staining. The scale bar represents 1  $\mu\text{m}$  on AFM and SEM-FEG images and 50  $\mu\text{m}$  on images from epifluorescence microscopy.

However, epifluorescence microscopy does not constitute a direct proof of bacteria viability or death.<sup>38</sup> Conversely, bacteria were also cultivated on an agar plate after having been in contact with the modified surfaces in order to count the actual number of bacterial colonies. A drastic decrease of  $\sim 45\%$  of bacterial growth was systematically observed after contact with SL-containing surfaces compared to the Au and Au-cys samples (Growth (%): Au = 100%, Au-cys = 95%, Au-cys-SL = 54%). These numbers are in very good agreement with the fluorescent staining (Intact bacteria (%): Au = 98%, Au-cys = 96%, Au-cys-SL = 58%) and confirm the antibacterial effect of SL-modified surfaces via membrane lysis. Note, in addition, that the rate of damaged bacteria stays constant over time from 1 h up to at least 6 h in contact with the surface. Similarly, we have found the same biocidal efficiency at different growth stages (exponential phase or stationary phase) of *L. ivanovii*.

**Understanding the Origin of Biocidal Effect of SL.** The data presented so far put in evidence several striking facts: (1) surface-grafted SL keep their biocidal action against Gram+ *Listeria ivanovii*; (2) the killing efficiency is in the 40–45% range; (3) the apparent mechanism of action occurs through membrane lysis, as described for the same compounds (and related glycolipids) in aqueous solutions.<sup>21–23,28</sup> The persistence of the antimicrobial properties of SL after their grafting onto a surface demonstrates that the carboxylic acid group may not play a key role in their antibacterial property, since the COOH is neutralized by the anchoring strategy. This is in line with the comparisons of lactone-type and acid-type sophorolipids activity in solution, which show that the former has a higher antimicrobial activity.<sup>28</sup>

To put in evidence the role of the sophorose unit, we have controlled the possible biocidal action of OA-grafted gold surface. In addition, to understand the potential role of the conformation of sophorose at the outer surface we have tested the biocidal action of the fully saturated form of acidic sophorolipids (SL<sub>0</sub>) and the corresponding fatty acid (SA), as shown in Figure 1. It is, in fact, known that the anomer conformations of synthetic glycolipids strongly influence their antibacterial activity in solution; for instance, the *alpha* anomer of the lauric ether derivative of methyl glucopyranoside has a MIC of 0.04 M, which is roughly 100 times smaller (hence, more efficient) than the corresponding *beta* anomer.<sup>31</sup> For these reasons, even if OA and SA are not supposed to have antibacterial effects in solution,<sup>24</sup> and since we are not aware of such properties for SL<sub>0</sub>, we have tested the MIC in solutions of these compounds. Using DMSO to improve solubility, and then diluting the solution in water, SL<sub>0</sub>, OA, and SA do not exhibit any inhibitory effect, even at high concentrations (32 mg/mL, i.e., 8-fold above the MIC value found in this work for SL, 4 mg/mL) and bacteria show their oval native shape and intact plasma membranes when observed by SEM-FEG (images not shown). Nevertheless, since SL<sub>0</sub> forms supramolecular water-insoluble fibers,<sup>34</sup> it is difficult to obtain reliable antibacterial data in solution and therefore the corresponding grafted surfaces appear as an interesting tool to explore the interactions between these molecules and bacteria.

OA, SA, and SL<sub>0</sub>-grafted surfaces have been elaborated and characterized following the same procedure as the one used for SL grafting (see description above): the corresponding infrared and XPS data (shown in Figures S3 and S4 in the Supporting Information) confirm the grafting of SL<sub>0</sub> on gold in equivalent amounts that SL (both layers have equivalent thickness,  $30.0 \pm 2.0$  Å for SL and  $31 \pm 5$  Å for SL<sub>0</sub>, according to the estimation based on XPS analyses, see Supporting Information) as well as OA and SA, making the comparison of antibacterial properties of these surfaces possible. Figure 4 displays the observations of bacteria deposit on these modified surfaces.

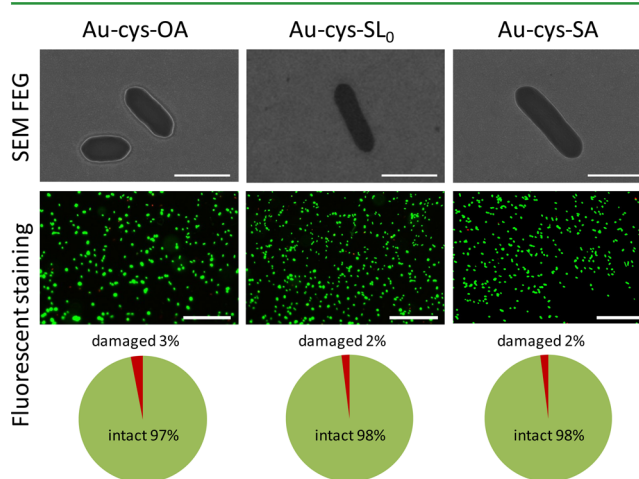


**Figure 4.** Bacteria (*L. ivanovii*) deposited on Au-cys-OA (left column), Au-cys-SL<sub>0</sub> (middle column), and Au-cys-SA (right column) surfaces observed by SEM-FEG (top range) and epifluorescence microscopy (bottom range). The charts below each image represent the percentage of adhering intact and damaged bacteria according to fluorescent staining. The scale bars represent 1  $\mu\text{m}$  on AFM images and 50  $\mu\text{m}$  on images from epifluorescence microscopy.

Bacteria exhibit their native oval shape on SEM images and look intact on all samples. The harmless features of these surfaces is confirmed by fluorescent staining: more than 97% of the adhered bacteria appear green after fluorescent staining, meaning that their membrane was not damaged by any of the tested compounds. The corresponding colony counting data after exposure are reported in Figure 5 (green bars); however,

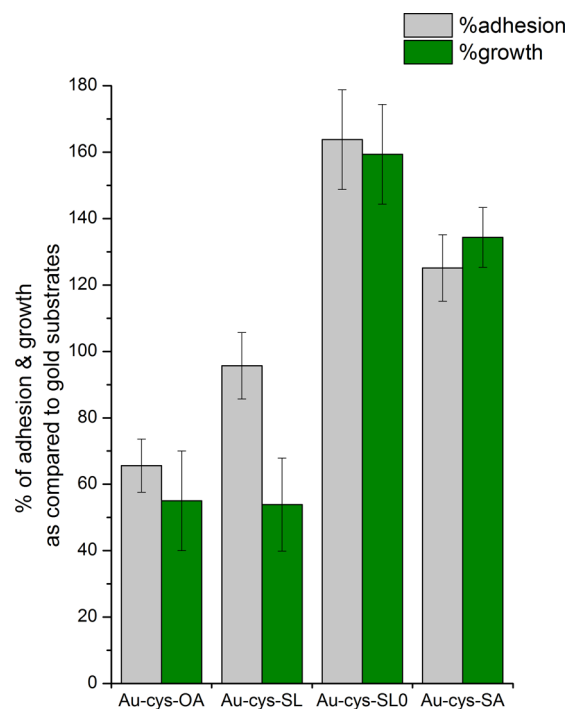


**Figure 5.** Adhesion (gray bars) and bacterial growth (green bars) of *Listeria ivanovii* after contact with Au-cys-OA, Au-cys-SL, Au-cys-SL<sub>0</sub>, and Au-cys-SA surfaces as compared to Au substrates.

these data must be weighted by the adhesion (% with respect to bare gold) of the bacteria onto the surfaces (gray bars in Figure 5). In fact, the adhesion capacity of *L. ivanovii* is not constant on all modified surfaces. When in contact with SL-modified surfaces, the bacterial adhesion is very similar (95–100%, within the experimental error bars) to what it is observed onto gold, but their growth is reduced by approximately 50%. This difference nicely confirms, from a quantitative point of view, the biocidal action of grafted SL, previously highlighted by fluorescent staining experiments, cf. Figure 4. Finally, the adhesive nature of SL<sub>0</sub> and, at a lower extent, the one of SA are higher than bare Au or SL surfaces (the adhesion on those surface being, respectively, estimated to 160 and 130% as compared to gold); the growth counting, which is found to be almost 60% and 30% higher with respect to gold for SL<sub>0</sub> and SA, respectively, is then solely attributed to the adhesive properties of these surfaces.

In order to better understand the interactions between bacteria and surfaces, water contact angles on the modified surfaces have been determined (Figure 6) as it may influence the contact between bacteria and surfaces and hence the biocidal effect.

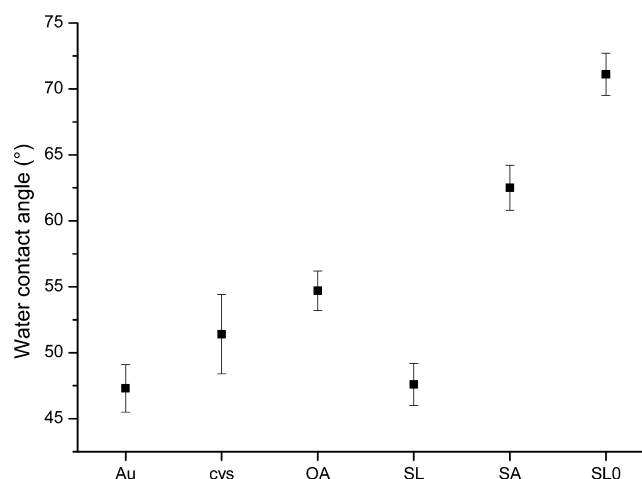


**Figure 6.** Water contact angle on bare gold surface and on functionalized surfaces.

The gold surface becomes more hydrophobic after functionalization with OA and SA, for which the water contact angles are respectively  $55^\circ \pm 2^\circ$  and  $62^\circ \pm 2^\circ$ . The sophorose units, hydroxyl-rich water-soluble disaccharides, of SL lead to an expected decrease of the contact angle with respect to OA from  $55^\circ \pm 2^\circ$  to  $48^\circ \pm 2^\circ$ , whereas the contact angle increases from  $62^\circ \pm 2^\circ$  to  $71^\circ \pm 2^\circ$  when passing from SA to SL<sub>0</sub>. The antinomic effect in terms of surface wettability between SL ( $48^\circ \pm 2^\circ$ ) and SL<sub>0</sub> ( $71^\circ \pm 2^\circ$ ) is unexpected, if one looks at the chemical nature of both quasi identical molecules. Nevertheless, this is not surprising; examples of conformational changes strongly affecting the wettability of coatings exist for peptides, where the chirality sense of the peptide backbone governs the hydrophilic/hydrophobic character of the coated surface.<sup>39</sup> It is also known that glucose-based surfaces/compounds can display different wettability properties. Cyclodextrins, for instance, are water-soluble compounds with a hydrophobic cavity,<sup>40</sup> as the orientation of the C–OH groups in glucose identifies regions of different water-loving properties.<sup>41</sup> A striking example is constituted by two allomorphs of cellulose, I<sub>α</sub> and I<sub>β</sub>, the (100) surfaces of which are, respectively, hydrophilic and hydrophobic.<sup>41</sup> The stronger wettability in I<sub>α</sub> was demonstrated to come from both the larger exposure of the C–OH groups of glucose and more prominent surface roughness while the glucose moieties of the I<sub>β</sub> are parallel to the surface (low roughness) and more C–OH groups are involved in hydrogen bonding with their close neighbors. In the case of SL-modified surfaces, we then believe that the double bond present in the SL molecule favors the preferential exposure of C–OH groups compared to the SL<sub>0</sub> coatings. Interestingly, if one lays SL and SL<sub>0</sub> molecules on a flat surface respecting the theoretical bond lengths, dihedral angles and chirality for both the sugar and C17 atom in the aliphatic chain, it is then possible to see that the actual orientation of the C–OH groups is orthogonal to the surface for SL, while it is parallel to it for SL<sub>0</sub>, as shown in Figure 7, and thus explaining the hydrophilicity of the SL-containing substrate if compared to the SL<sub>0</sub> substrate. In addition, the bending of the SL molecule may increase local disorder and a loss of molecular packing, similarly to differences of molecular packing and water-solubility encountered in solution: at room temperature and under acidic conditions, SL forms micelles (water-soluble) while SL<sub>0</sub> forms water-insoluble crystalline fibers with nanoscale chirality.<sup>34</sup>

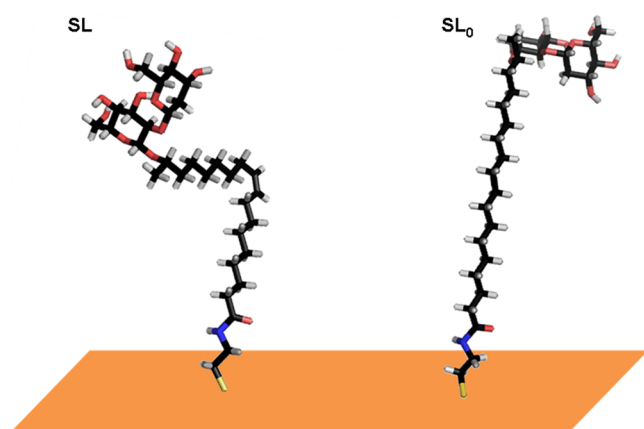


**Figure 7.** SL (left) and SL<sub>0</sub> (right) lying on top of a model surface (oxygen, red; hydrogen, white; sulfur, yellow; nitrogen, green).

## DISCUSSION

By comparing the bacteria morphology and viability on OA, SA, SL<sub>0</sub>, and SL grafted samples, one can safely assert that only surfaces with the unsaturated form of sophorolipids have a biocidal activity (to this regard, please also see the comment in the PM-RAIRS section, page 4, of the [Supporting Information](#)). The simultaneous presence of the hydrophilic sophorose group and the double bond appear to be necessary to induce bacterial killing. These two structural features have also a crucial influence on several physicochemical properties. Sophorose is a bulky disaccharide and its steric hindrance influences the conformation of SL: the surface exhibits a loose packing as observed for antimicrobial peptides chemically grafted on thiolated self-assembled monolayers, for instance.<sup>35</sup> The presence of the double bond induces curvature in the alkyl chain layer, thus contributing to the loose, probably defect-rich, packing of the SL compound. The orientation of sophorose is also directly related to the constraints imposed by the C=C double bond (120° angle), and so is influencing the intermolecular hydrogen bonding network. The use of a fully saturated (stearic) alkyl chain in SL<sub>0</sub> has several important consequences; it is in fact known that molecular packing is tighter for stearic acid based compound.<sup>42</sup> The so different values of the water contact angles of Au-cys-SL and Au-cys-SL<sub>0</sub> suggest that the orientation of the sophorose is different on gold, maybe correlated to the so different biocidal properties (40–50% of damaged bacteria on SL modified-surfaces compared to almost none on SL<sub>0</sub> modified-surfaces). Consequently, a variability of the killing-by-contact efficiency could be due to two combined reasons: the disaccharide orientation and local disorder.

To understand the importance of these findings, one must recall the role of carbohydrates in biocidal compounds, often mentioned but never clarified. In the first place, the biocidal properties of glycolipids have always been found for free molecules in solution, where it is impossible to dissociate the action of the sugar from its covalently bonded backbone. Nevertheless, some works show that the efficiency against a given organism depends on the nature of the sugar. For instance, sucrose monolaurate is less effective toward *Enterococcus faecalis* than lactose monolaurate, but their activities are comparable toward *Listeria monocytogenes*.<sup>43,44</sup> Besides, a stronger piece of evidence that the nature of the carbohydrate has an important role was reported by Nobmann et al. on the

effect of *alpha* or *beta* anomer on the MIC, as discussed previously.<sup>31</sup>

When polysaccharides or sugars are grafted on a surface, the main reported effect concerns the enhancement, or reduction, of microorganisms adhesion but no biocidal effect.<sup>19</sup> The decrease of bacterial viability observed on gold samples modified with monounsaturated sophorolipids suggests a killing-by-contact action related to the presence of covalently grafted molecules, whereas the hypothetical role of micelles is excluded, since the initial sophorolipid concentration is of 50  $\mu\text{g mL}^{-1}$ , a value which is well below the critical micelle concentration ( $\sim 110 \mu\text{g mL}^{-1}$ ).<sup>45</sup> In addition, as shown by quartz crystal microbalance experiments, the grafted layer remains stable after the rinsing procedure performed at the end of the grafting (cf. Figure S2 in the [Supporting Information](#)). In any case, even if all sophorolipids present at the gold surface after rinsing ( $\sim 180 \text{ ng}$  according to QCM experiments, as exposed in the [Supporting Information](#)) are released into the 100  $\mu\text{L}$  drop of bacterial suspension used in the antibacterial tests, the concentration would be less than 2  $\mu\text{g mL}^{-1}$ , thus assuring to be below the typical MIC and the MBC for free sophorolipids (respectively, 4 and 32  $\text{mg mL}^{-1}$ , as measured in this study). Excluding the hypothesis according to which bacteria may be killed by residual free sophorolipid molecules, it also automatically excludes the fact that grafted sophorolipids act via the classical “surfactant effect”, as described in solution for many other glycolipids and more in general surfactant molecules or even peptides.<sup>21–23,28,46</sup> Here SL can only interfere with the bacterial cell envelope through the sophorose moiety, which is not able to diffuse neither through the cell wall nor the plasma membrane. We also make the assumption that sophorolipids, characterized by an ether covalent bond between sophorose and oleic acid (ether-based glycolipids are known to be stable during their antibacterial activity<sup>31</sup>), are stable at the gold surface toward potential hydrolysis by bacterial esterase. Another favorable argument consists in the fact that if sophorolipids would be hydrolyzed by *L. ivanovii*, we would not expect an antibacterial activity at all, as the residual oleic acid moiety has none. The killing process is then directly related to the contact between the cell envelope and the sophorose headgroup. Moreover, there is a general consensus on the fact that the most effective biocidal chemical groups (e.g., antimicrobial peptides, alkylammonium derivatives) are able to approach and pierce the cell wall thanks to their rigid and electrically charged nature. The action of cationic polymers for instance is usually described as disrupting the lipidic membranes of bacteria through electrostatic and hydrophobic interactions.<sup>47</sup> Similar mechanisms are also suggested for antimicrobial peptides.<sup>25</sup> In comparison, because of their electroneutrality, monounsaturated sophorolipids have little chance to cause membrane lysis after grafting. We believe that the origin of their biocidal effect is rather related to specific sophorose/cell envelope interactions. However, these have never been described in the literature.

To understand the origin of cell envelope damage in our system, we thus make two hypotheses, biochemical and/or biophysical (or both simultaneously). The biochemical pathway refers to a possible interaction between sophorose and the microorganism which triggers a (series of) biochemical response(s) responsible for the cell envelope rupture. This is the classical way penicillin antibiotics work by inhibiting the transpeptidase, enzymes responsible for the cross-linking of the peptidoglycan layer.<sup>48</sup> Similar arguments are also used to

explain the mechanism of action of the moenomycin antibiotic, a well-known glycolipid, and its derivatives. They inhibit the *in vitro* transglycosylation reaction in *E. coli*, thus blocking the synthesis of the cell wall and its eventual death, with or without lysis.<sup>49–51</sup> In addition, a potential role as signaling molecules that regulate gene expression has been discussed to explain the antiadhesive properties of some bacterial exopolysaccharides.<sup>16</sup> If these specific mechanisms do not seem to be applicable to the case of surface-grafted SL against *Listeria* (since it seems difficult for anchoring SL to interfere with the inner metabolism of the bacteria), similar sophorose-induced biochemical pathways may not be completely excluded, even though unknown at the moment. The biophysical pathway refers to a mechanical, destabilizing interaction between the carbohydrate and the *Listeria* cell envelope, which is mainly constituted by a peptidoglycan and phospholipid layers.<sup>52,53</sup> If the action of sophorose on the cell envelope is out of doubt, the way such interaction occurs is still unknown. Specific literature data neither exist on this specific system nor, to the best of our knowledge, on the more general destabilization process of the peptidoglycan layer by mono- and disaccharides. As far as an action on the plasma membrane, the lysis of which is put in evidence here by the epifluorescence observations (if PI reaches the nucleic acid of red bacteria, it means their plasma membrane is damaged), one could formulate two different mechanistic hypotheses, admitting the previous interpenetration of the cell wall: (1) intramembrane sugar intercalation,<sup>54–56</sup> perturbing the local liquid crystalline order, as observed in the case of other nonreducing disaccharides (e.g., trehalose and sucrose).<sup>32</sup> (2) Mediated membrane destabilization, as shown by recent fundamental studies by Abbott et al. go in this sense, showing the destabilizing effects the macromolecular adsorbents of biological relevance (e.g., proteins) may have on model phospholipid liquid crystal membranes.<sup>57</sup> They have shown that not only weak binding of proteins drive the reorganization of the phospholipids and trigger orientational transitions in the liquid crystals but also that similar events can also occur by ligand (biotin)-receptor (streptavidin) recognition phenomena, where streptavidin is contained in the liquid crystal layer and biotin in an external phospholipid vesicles approaching it.<sup>58</sup> It is not known at the moment if any of these hypotheses, generally formulated in the case of interactions between free molecules and a cell envelope, can be applied to the present biocidal effect of surfaces-grafted sophorolipids and it deserves more fundamental studies. Besides, whatever the mechanism, the main reason for which the saturated SL<sub>0</sub> sophorolipid does not seem to have any biocidal property could be multiple: poor accessibility of individual surface sophorose groups, enhanced bacterial adhesion, both limiting the accessibility of sophorose and consequent interaction with membrane penetration.

## CONCLUSION

This paper reports the conception of an innovative biocidal coatings using carbohydrates immobilized on a surface. Sophorolipids, yeast-derived bolaform biosurfactants, were successfully attached to a model flat gold surface modified by a thiolamine primer through amidation of their COOH group. The resulting glycosylated surface, where sophorose (glucose  $\beta(1,2)$ ), a nonreducing disaccharide, lays on top of the surface, shows a biocidal activity toward *Listeria ivanovii* bacteria. So far, glycosylated surfaces have been known for their antiadhesive properties. A combination of microscopy tools shows that

bacteria are killed through membrane lysis. Bacterial growth and adhesive tests show that between 40% and 50% of exposed bacteria are damaged; these values are coherent with the quantitative data obtained from fluorescent staining. To better understand the mechanism of action, the effect of sophorolipids was compared to rational molecular variations of this compound: oleic acid, constituting the aliphatic backbone of sophorolipids, fully saturated sophorolipids and stearic acid, the aliphatic component of the latter, have been grafted on gold and no biocidal activity could be detected. This comparative study then underlines the crucial role played by sophorose but it also highlights the importance of the aliphatic chain configuration, influencing the substrate wettability, bacterial adhesion, and biocidal effects. If this first example of a biocidal effect from a glycan array demonstrates the membrane disrupting properties of a nonreducing disaccharide, the actual mechanism of interaction between sophorose and the bacterial membrane is still unknown, and it may not still be confined to this particular sugar alone.

## ASSOCIATED CONTENT

### Supporting Information

The Supporting Information is available free of charge on the ACS Publications website at DOI: 10.1021/acsami.5b05090.

Detailed XPS, QCM, and PM-RAIRS additional data and analyses of SL, SL<sub>0</sub>, OA, and SA on Au-cys substrates (PDF)

## AUTHOR INFORMATION

### Corresponding Authors

\*E-mail: niki.baccile@upmc.fr.

\*E-mail: vincent.humblot@upmc.fr.

### Funding

This work was supported by French state funds managed by the ANR within the Investissements d'Avenir program under Reference ANR-11-IDEX-0004-02 and more specifically within the framework of the Cluster of Excellence MATISSE.

### Notes

The authors declare no competing financial interest.

## ACKNOWLEDGMENTS

The authors acknowledge IMPC (Institut des Matériaux de Paris Centre, FR2482) and the C'Nano projects of the Region Ile-de-France, for SEM-FEG and Omicron XPS apparatus funding. Christophe Méthivier is deeply acknowledged for his important help in XPS calculations. Frederik Tielens (LCMCP, Université Pierre et Marie Curie, Paris, France) is kindly acknowledged for his help with the molecular drawing. Bastien Wild (LHYGES, Université de Strasbourg, France) is kindly acknowledged for his initial help in the experimental part.

## REFERENCES

- (1) Hall-Stoodley, L.; Costerton, J. W.; Stoodley, P. Bacterial Biofilms: From the Natural Environment to Infectious Diseases. *Nat. Rev. Microbiol.* **2004**, *2*, 95–108.
- (2) Costerton, J. W.; Lewandowski, Z.; Caldwell, D. E.; Korber, D. R.; Lappin-Scott, H. M. Microbial Biofilms. *Annu. Rev. Microbiol.* **1995**, *49*, 711–745.
- (3) Klevens, R. M.; Edwards, J. R.; Richards, C. L.; Horan, T. C.; Gaynes, R. P.; Pollock, D. A.; Cardo, D. M. Estimating Health Care-Associated Infections and Deaths in U.S. Hospitals, 2002. *Public Health Rep.* **2007**, *122*, 160–166.



- (4) Lewis, K. Multidrug Tolerance of Biofilms and Persister Cells. *Curr. Top. Microbiol.* **2008**, *322*, 107–131.
- (5) Tiller, J. C.; Liao, C. J.; Lewis, K.; Klivanov, A. Designing Surfaces That Kill Bacteria on Contact. *Proc. Natl. Acad. Sci. U. S. A.* **2001**, *98*, 5981–5985.
- (6) Cado, G.; Aslam, R.; Séon, L.; Garnier, T.; Fabre, R.; Parat, A.; Chassepot, A.; Voegel, J. C.; Senger, B.; Schneider, F.; Frère, Y.; Jierry, L.; Schaaf, P.; Kerdjoudj, H.; Metz-Boutigue, M. H.; Boulmedais, F. Self-Defensive Biomaterial Coating against Bacteria and Yeasts: Polysaccharide Multilayer Film with Embedded Antimicrobial Peptide. *Adv. Funct. Mater.* **2013**, *23*, 4801–4809.
- (7) Aumsuwan, N.; Heinhorst, S.; Urban, M. W. The Effectiveness of Antibiotic Activity of Penicillin Attached to Expanded Poly-(Tetrafluoroethylene) (Eptfe) Surfaces: A Quantitative Assessment. *Biomacromolecules* **2007**, *8*, 3525–3530.
- (8) Lee, D.; Cohen, R. E.; Rubner, M. F. Antibacterial Properties of Ag Nanoparticle Loaded Multilayers and Formation of Magnetically Directed Antibacterial Microparticles. *Langmuir* **2005**, *21*, 9651–9.
- (9) Rocha, M.; Ferreira, F. A.; Souza, M. M.; Prentice, C. Antimicrobial Films: A Review. In *Microbial Pathogens and Strategies for Combating Them: Science, Technology and Education*; A. Méndez-Vilas, A., Ed. Formatex Research Center:: Extremadura, Spain, 2013; Vol. 1, pp 23–31.
- (10) Glinel, K.; Thébault, P.; Humblot, V.; Pradier, C.-M.; Jouenne, T. Antibacterial Surfaces Developed from Bio-Inspired Approaches. *Acta Biomater.* **2012**, *8*, 1670–1684.
- (11) Osborn, H. M.; Evans, P. G.; Gemmill, N.; Osborne, S. D. Carbohydrate-Based Therapeutics. *J. Pharm. Pharmacol.* **2004**, *56*, 691–702.
- (12) Laurent, N.; Voglmeier, J.; Flitsch, S. L. Glycoarrays—Tools for Determining Protein-Carbohydrate Interactions and Glycoenzyme Specificity. *Chem. Commun.* **2008**, 4400–12.
- (13) Cortes-Sanchez, A. d. J.; Hernandez-Sanchez, H.; Jaramillo-Flores, M. E. Biological Activity of Glycolipids Produced by Microorganisms: New Trends and Possible Therapeutic Alternatives. *Microbiol. Res.* **2013**, *168*, 22–32.
- (14) Valle, J.; Da Re, S.; Henry, N.; Fontaine, T.; Balestrino, D.; Latour-Lambert, P.; Ghigo, J. M. Broad-Spectrum Biofilm Inhibition by a Secreted Bacterial Polysaccharide. *Proc. Natl. Acad. Sci. U. S. A.* **2006**, *103*, 12558–63.
- (15) Brajtburg, J.; Powderly, W. G.; Kobayashi, G. S.; Medoff, G. Amphotericin B: Current Understanding of Mechanisms of Action. *Antimicrob. Agents Chemother.* **1990**, *34*, 183–188.
- (16) Bernal, P.; Llamas, M. A. Promising Biotechnological Applications of Antibiofilm Exopolysaccharides. *Microb. Biotechnol.* **2012**, *5*, 670–673.
- (17) Fessele, C.; Lindhorst, T. K. Effect of Aminophenyl and Aminothiahexyl A-D-Glycosides of the Manno-, Gluco-, and Galacto-Series on Type 1 Fimbriae-Mediated Adhesion of *Escherichia Coli*. *Biology* **2013**, *2*, 1135–1149.
- (18) Hartmann, M.; Horst, A. K.; Klemm, P.; Lindhorst, T. K.; Hartmann, M.; Horst, A. K.; Klemm, P.; Lindhorst, T. K. A Kit for the Investigation of Live *Escherichia Coli* Cell Adhesion to Glycosylated Surfaces. *Chem. Commun.* **2010**, *46*, 330–332.
- (19) Kesel, S.; Mader, A.; Seeberger, P. H.; Lieleg, O.; Opitz, M. Carbohydrate Coating Reduces Adhesion of Biofilm-Forming *Bacillus Subtilis* to Gold Surfaces. *Appl. Environ. Microbiol.* **2014**, *80*, 5911–5917.
- (20) Wehner, J. W.; Hartmann, M.; Lindhorst, T. K. Are Multivalent Cluster Glycosides a Means of Controlling Ligand Density of Glycoarrays? *Carbohydr. Res.* **2013**, *371*, 22–31.
- (21) Chapman, J.; Diehl, M.; Lyman, R. Biocide Susceptibility and Intracellular Glutathione in *Escherichia Coli*. *J. Ind. Microbiol.* **1993**, *12*, 403–407.
- (22) Glover, R. E.; Smith, R. R.; Jones, M. V.; Jackson, S. K.; Rowlands, C. C. An Epr Investigation of Surfactant Action on Bacterial Membranes. *FEMS Microbiol. Lett.* **1999**, *177*, 57–62.
- (23) Lang, S.; Katsiwela, E.; Wagner, F. Antimicrobial Effects of Biosurfactants. *Fett/Lipid* **1989**, *91*, 363–366.
- (24) Kabara, J. J.; Swieczkowski, D. M.; Conley, A. J.; Truant, J. P. Fatty Acids and Derivatives as Antimicrobial Agents. *Antimicrob. Agents Chemother.* **1972**, *2*, 23–28.
- (25) Brogden, K. A. Antimicrobial Peptides: Pore Formers or Metabolic Inhibitors in Bacteria? *Nat. Rev. Microbiol.* **2005**, *3*, 238–250.
- (26) Hurdle, J. G.; O'Neill, A. J.; Chopra, I.; Lee, R. E. Targeting Bacterial Membrane Function: An Underexploited Mechanism for Treating Persistent Infections. *Nat. Rev. Microbiol.* **2011**, *9*, 62–75.
- (27) Baek, S. H.; Sun, X. X.; Lee, Y. J.; Wang, S. Y.; Han, K. N.; Choi, J. K.; Noh, J. H.; Kim, E. K. Mitigation of Harmful Algal Blooms by Sophorolipid. *J. Microbiol. Biotechnol.* **2003**, *13*, 651–659.
- (28) Kim, K.; Dalsoo, Y.; Youngbum, K.; Baekseok, L.; Doonhoon, S.; Eun-Ki, K. Characteristics of Sophorolipid as an Antimicrobial Agent. *J. Microbiol. Biotechnol.* **2002**, *12*, 235–241.
- (29) Van Bogaert, I. N. A.; Zhang, J.; Soetaert, W. Microbial Synthesis of Sophorolipids. *Process Biochem.* **2011**, *46*, 821–833.
- (30) Mukherjee, S.; Das, P.; Sen, R. Towards Commercial Production of Microbial Surfactants. *Trends Biotechnol.* **2006**, *24*, 509–515.
- (31) Nobmann, P.; Smith, A.; Dunne, J.; Henehan, G.; Bourke, P. The Antimicrobial Efficacy and Structure Activity Relationship of Novel Carbohydrate Fatty Acid Derivatives against *Listeria Spp.* And Food Spoilage Microorganisms. *Int. J. Food Microbiol.* **2009**, *128*, 440–5.
- (32) Moiset, G.; Lopez, C. A.; Bartelds, R.; Syga, L.; Rijpkema, E.; Cukkemane, A.; Baldus, M.; Poolman, B.; Marrink, S. J. Disaccharides Impact the Lateral Organization of Lipid Membranes. *J. Am. Chem. Soc.* **2014**, *136*, 16167–75.
- (33) Baccile, N.; Cuvier, A.-S.; Valotteau, C.; Van Bogaert, I. N. A. Practical Methods to Reduce Impurities for Gram-Scale Amounts of Acidic Sophorolipid Biosurfactants. *Eur. J. Lipid Sci. Technol.* **2013**, *115*, 1404–1412.
- (34) Cuvier, A.-S.; Berton, J.; Stevens, C. V.; Fadda, G. C.; Babonneau, F.; Van Bogaert, I. N.; Soetaert, W.; Pehau-Arnaudet, G.; Baccile, N. Ph-Triggered Formation of Nanoribbons from Yeast-Derived Glycolipid Biosurfactants. *Soft Matter* **2014**, *10*, 3950–3959.
- (35) Yala, J.-F.; Thébault, P.; Héquet, A.; Humblot, V.; Pradier, C.-M.; Berjeaud, J.-M. Elaboration of Antibiofilm Materials by Chemical Grafting of an Antimicrobial Peptide. *Appl. Microbiol. Biotechnol.* **2011**, *89*, 623–634.
- (36) Robichon, D.; Girard, J.-C.; Cenatiempo, Y.; Cavellier, J.-F. Atomic Force Microscopy Imaging of Dried or Living Bacteria. *C. R. Acad. Sci., Ser. III* **1999**, *322*, 687–693.
- (37) Azim, A.; Shah, V.; Doncel, G. F.; Peterson, N.; Gao, W.; Gross, R. Amino Acid Conjugated Sophorolipids: A New Family of Biologically Active Functionalized Glycolipids. *Bioconjugate Chem.* **2006**, *17*, 1523–1529.
- (38) Roszak, D. B.; Colwell, R. R. Survival Strategies of Bacteria in the Natural Environment. *Microbiol. Rev.* **1987**, *51*, 365–379.
- (39) Qing, G.; Sun, T. Chirality-Driven Wettability Switching and Mass Transfer. *Angew. Chem., Int. Ed.* **2014**, *53*, 930–932.
- (40) Martinez, A.; Ortiz Mellet, C.; Garcia Fernandez, J. M. Cyclodextrin-Based Multivalent Glycodisplays: Covalent and Supramolecular Conjugates to Assess Carbohydrate-Protein Interactions. *Chem. Soc. Rev.* **2013**, *42*, 4746–4773.
- (41) Hoja, J.; Maurer, R. J.; Sax, A. F. Adsorption of Glucose, Cellobiose, and Cellotetraose onto Cellulose Model Surfaces. *J. Phys. Chem. B* **2014**, *118*, 9017–9027.
- (42) Small, D. M. Lateral Chain Packing in Lipids and Membranes. *J. Lipid Res.* **1984**, *25*, 1490–1500.
- (43) Devulapalle, K. S.; Gomez de Segura, A.; Ferrer, M.; Alcalde, M.; Mooser, G.; Plou, F. J. Effect of Carbohydrate Fatty Acid Esters on *Streptococcus Sobrinus* and Glucosyltransferase Activity. *Carbohydr. Res.* **2004**, *339*, 1029–34.
- (44) Wagh, A.; Shen, S.; Shen, F. A.; Miller, C. D.; Walsh, M. K. Effect of Lactose Monolaurate on Pathogenic and Nonpathogenic Bacteria. *Appl. Environ. Microbiol.* **2012**, *78*, 3465–8.

- (45) Imura, T.; Masuda, Y.; Minamikawa, H.; Fukuoka, T.; Konishi, M.; Morita, T.; Sakai, H.; Abe, M.; Kitamoto, D. Enzymatic Conversion of Diacetylated Sophorolipid into Acetylated Glucose-lipid: Surface-Active Properties of Novel Bolaform Biosurfactants. *J. Oleo Sci.* **2010**, *59*, 495–501.
- (46) Bechinger, B.; Lohner, K. Detergent-Like Actions of Linear Amphipathic Cationic Antimicrobial Peptides. *Biochim. Biophys. Acta, Biomembr.* **2006**, *1758*, 1529–1539.
- (47) Siedenbiedel, F.; Tiller, J. C. Antimicrobial Polymers in Solution and on Surfaces: Overview and Functional Principles. *Polymers* **2012**, *4*, 46–71.
- (48) Yocum, R. R.; Rasmussen, J. R.; Strominger, J. L. The Mechanism of Action of Penicillin. Penicillin Acylates the Active Site of *Bacillus Stearothermophilus* D-Alanine Carboxypeptidase. *J. Biol. Chem.* **1980**, *255*, 3977–3986.
- (49) Baizman, E. R.; Branstrom, A. A.; Longley, C. B.; Allanson, N.; Sofia, M. J.; Gange, D.; Goldman, R. C. Antibacterial Activity of Synthetic Analogues Based on the Disaccharide Structure of Moenomycin, an Inhibitor of Bacterial Transglycosylase. *Microbiology* **2000**, *146*, 3129–3140.
- (50) Van Heijenoort, Y.; Derrien, M.; Van Heijenoort, J. Polymerization by Transglycosylation in the Biosynthesis of the Peptidoglycan of *Escherichia Coli* K 12 and Its Inhibition by Antibiotics. *FEBS Lett.* **1978**, *89*, 141–144.
- (51) Van Heijenoort, Y.; Van Heijenoort, J. Biosynthesis of the Peptidoglycan of *Escherichia Coli* K-12: Properties of the *in Vitro* Polymerization by Transglycosylation. *FEBS Lett.* **1980**, *110*, 241–244.
- (52) Ghosh, B. K.; Carroll, K. K. Isolation, Composition, and Structure of Membrane of *Listeria Monocytogenes*. *J. Bacteriol.* **1968**, *95*, 688–699.
- (53) Vazquez-Boland, J. A.; Kuhn, M.; Berche, P.; Chakraborty, T.; Dominguez-Bernal, G.; Goebel, W.; Gonzalez-Zorn, B.; Wehland, J.; Kreft, J. *Listeria* Pathogenesis and Molecular Virulence Determinants. *Clinical Microbiol. Rev.* **2001**, *14*, 584–640.
- (54) Crowe, J. H.; Whittam, M. A.; Chapman, D.; Crowe, L. M. Interactions of Phospholipid Monolayers with Carbohydrates. *Biochim. Biophys. Acta, Biomembr.* **1984**, *769*, 151–9.
- (55) Lenné, T.; Bryant, G.; Holcomb, R.; Koster, K. L. How Much Solute Is Needed to Inhibit the Fluid to Gel Membrane Phase Transition at Low Hydration? *Biochim. Biophys. Acta, Biomembr.* **2007**, *1768*, 1019–1022.
- (56) Andersen, H. D.; Wang, C.; Arleth, L.; Peters, G. H.; Westh, P. Reconciliation of Opposing Views on Membrane–Sugar Interactions. *Proc. Natl. Acad. Sci. U. S. A.* **2011**, *108*, 1874–1878.
- (57) Brake, J. M.; Daschner, M. K.; Luk, Y. Y.; Abbott, N. L. Biomolecular Interactions at Phospholipid-Decorated Surfaces of Liquid Crystals. *Science* **2003**, *302*, 2094–2097.
- (58) Tan, L. N.; Orler, V. J.; Abbott, N. L. Ordering Transitions Triggered by Specific Binding of Vesicles to Protein-Decorated Interfaces of Thermotropic Liquid Crystals. *Langmuir* **2012**, *28*, 6364–6376.